Metal mobility in the groundwater of a paddy field in Camargue (South eastern France)

L. Cary [a,*], F. Trolard [b]

[a] *Dept. Solos e Nutrição de plantas e nutrição de plantas, NUPEGEL, ESALQ/USP, Avenida Pádua Dias, 11, Caixa postal 9, 13418-900 Piracicaba - SP, Brazil*
[b] *INRA, UR Géochimie des sols et des eaux, Europôle de l'Arbois BP 80, 13545 Aix-en-Provence, cedex 4, France*

Abstract

Waterlogged soils are submitted to temporal variations of aeration and aerobic–anaerobic conditions which influence redox conditions and thus element mobility. Cultivated paddy soils, that are an accurate redox-dynamic environment, can be found in Camargue (Rhône deltaic plain, SE France). In order to monitor fast physical and chemical variations in the waterlogged soil, a multiparametric probe was chosen to acquire continuous and *in situ* data. It can be showed that (i) Eh variations happen at quasi-constant pH during Mediterranean storms in non-irrigated seasons, and induce sharp variations of Fe(II) and Mn concentrations, and (ii) the soil is saturated with water under anaerobic conditions during long periods, where sharp pH fluctuations controlled by $p\text{CO}_2$ evolution affect redox processes. During irrigation periods, Fe and Mn precipitate as oxides or co-precipitate with Al, Mg and Si at depth. These neoformed phases however can be dissolved when irrigation stops. The understanding of the reactions of the system, under varying conditions, is important in order to better assess its durability and anticipate the consequences of soil use or agricultural practices changes.
© 2007 Elsevier B.V. All rights reserved.

Keywords: Metal mobility; Dissolved iron; Redox potential; Groundwater; Paddy field; Camargue

1. Introduction

Iron in soil is one of the five most important chemical elements in abundance. By decreasing order of abundance, iron minerals found in soils are iron oxides, clay minerals, iron sulphides and carbonates (Stucki, 1988). Iron oxides play a major role in biogeochemical cycles of C, N and S in soils and sediments as electron donor and acceptor in oxido-reduction processes. They also influence the mobility of many trace metals acting as host minerals. The mobility of Fe is thus important in soil genesis (Schwertann, 1988), ore accumulation, and biogeochemical processes studied through soil solution (Ponnamperuma, 1972), either directly through its abundance and properties, or indirectly in redox processes. In order to quantify the host role of iron oxides, selective extraction may be carried out (Trolard, 1993; Trolard et al., 1995).

In anaerobic conditions, the final electron acceptor are, by order of decreasing oxido-reductive potential: nitrate ion (denitrification), manganese oxides, iron oxides, sulphate ion and CO_2 (formation of methane), (Turner and Patrick, 1968; Ponnamperuma, 1972; Sposito, 1981). In hydromorphic soils, Fe(III) in oxides is one of the largest

* Corresponding author.
E-mail addresses: lisecary@gmail.com (L. Cary),
trolard@aix.inra.fr (F. Trolard).

contributors to soil oxidation capacity when oxygen is absent (Kirk, 2004). Seasonal variations of redox conditions are illustrated by alternations of oxidation of Fe^{2+} in Fe^{3+} or reduction of Fe^{3+} in Fe^{2+}; oxido-reductive dynamics induce temporal oscillations of the Fe oxidation state (Van Cappellen et al., 1998). The great difference of mobility between Fe^{2+}, soluble and Fe^{3+}, mostly insoluble, leads to iron segregation in soil horizons or soil sequences. In strong oxidizing conditions, Fe-oxides such as goethite, lepidocrocite or hematite predominate whereas in strong reducing conditions, Fe sulfides precipitate. However, in moderately reducing conditions, aqueous Fe is controlled by equilibrium with a mixed green rust (Ponnamperuma, 1972; Bourrié et al., 1999) now known as fougerite (Féder, 2005).

The mobility of elements in paddy soils has been the subject of countless works, especially in the contexts of natural or anthropic polluted soils or groundwaters. The most recent and significant example is the amount of studies about the contamination of groundwaters, soil and rice by As in Bangladesh (an overview has been made by Hossain (2006) and references herein; Meharg (2004), Van Geen et al. (2006), Polizzotto et al. (2006)…). Nevertheless, only few studies are based on continuous and *in situ* data acquisition to better assess the impact of alternations of oxidative and reductive conditions on metal mobility (Ponnamperuma et al., 1967; Ponnamperuma, 1972; Jaffrezic, 1997; Trolard et al., 1998; Boivin et al., 2002; Féder et al., 2005; Cary and Trolard, 2006). Precisely, the importance of high frequency analyses of the groundwater quality is rarely pointed out although it

allows to studying daily variations or long term evolution. Consequently, physical and chemical analyses were made *in situ* at high frequency, in order to determine the impact of aerobic and anaerobic alternations on the mobility of metals in waterlogged soils.

2. Material and methods

2.1. Studied area

The Camargue is the Rhône deltaic plain in South eastern France. It is essentially modelled by fluvial ramblings and ramifications, and by marine deposits. Soils are usually submitted to hydromorphy and salinisation by evaporation of shallow groundwaters which leads to salt precipitation. During the last 30 years, a large area of Camargue has been fitted for rice cultivation in order to limit evaporation and salt precipitation by large inputs of fresh waters.

The studied area is located in Camargue, North-West of the Vaccarès Lagoon (Fig. 1). The studied soils are composed of fluvial sediments, which were deposited by the paleo-Rhône (Astier, 1970) called the Saint-Ferréol Channel (L'homer et al., 1981). The activity of this channel lasted from 5.500 BP to the end of the XVth Century (Rossiaud, 1994). The dimensions of the paleochannel are 500 m large for a maximum of 15 m depth. The fluvial clayed–silty–sandy sediments constitute an aquifer with fresh waters. On the contrary, the surrounding sediments not belonging to the paleochannel contain salted waters (Revil et al., 2005). Before
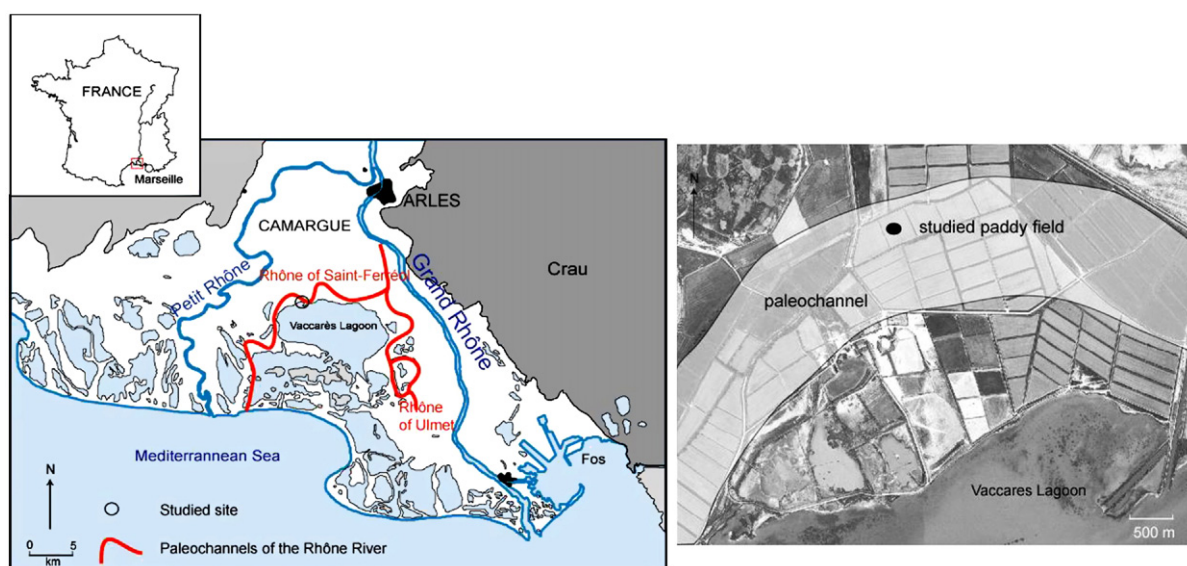

Fig. 1. The Camargue and the studied site in the South East of France.

1978, the site was mostly a non-irrigated meadow. From 1978 to 2004, rice has been cultivated, except in 2002 when wheat was cropped.

Paddy soils are continuously submerged from mid-April to the end of August, with a time-growing height of water. Irrigation water comes from the Rhône River through a scheme of channeling. Between 4000 and 7000 m³ of water per hectare cross the soil profile per year (Chauvelon, 1996; Heurteaux, 1990). A plough sole is created to maintain flooded conditions in the topsoil. The paddy soil is a hydragric anthrosol (FAO, 1999) and its description can be found in Cary and Trolard (2006). HCl reactivity occurs at all depths indicating a carbonated system. Bulk analyses were made after acid dissolution on total at the CNRS-CRPG (Vandoeuvre-les-Nancy). The concentrations of major and minor elements such as Al, Ca, Fe, Mn, Ti, Mg and Cu are larger in the 50–110 cm zone than in the other horizons (Fig. 2). The Si content in this zone decreases along with the decrease of the sand fraction and the increase of the clay fraction.

2.2. In situ soil solution study

A multiparametric probe designed for oceanic measurements in seawater is used. The probe was adapted to measure *in situ* and every hour physico-chemical parameters as temperature (T, °C), electric conductivity (EC, mS/cm), pH and the oxido-reduction potential (Eh, mV) in the soil solution (Féder et al., 2005). Measures were performed almost every week at 1.1 m depth in the waterlogged soil during Autumn 2002 and then at 1.6 m depth during Summer 2003. The water table level is measured in a piezometer situated 1 m far from the probe.

The oxido-reduction potential is measured with a platinum electrode against standard Ag/AgCl electrode and is converted to the normal hydrogen scale (NHE)
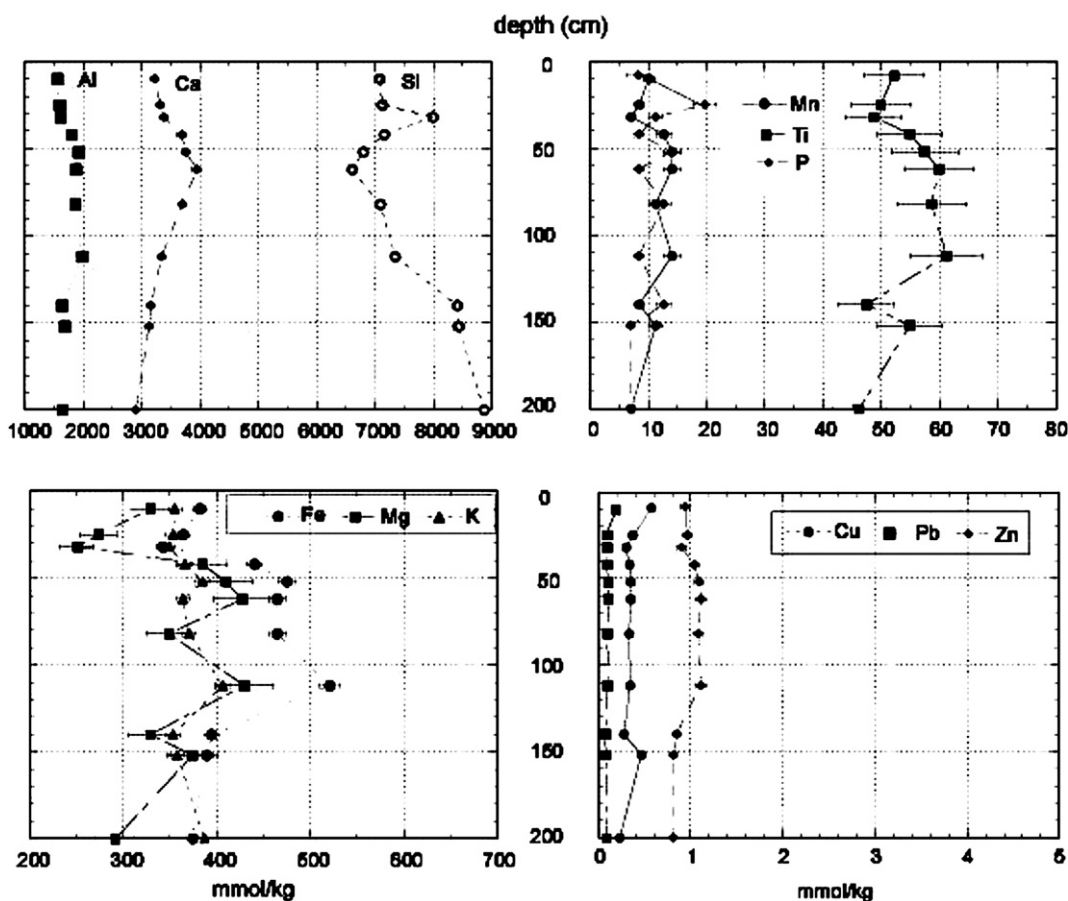

Fig. 2. Total analysis obtained after acid digestion of bulk samples from the paddy soil.

Table 1
Values of solubility products at 298.15 K and 1 bar

Mineral	log K
Pyrite	7.49 [a]
Mackinawite	−4.2 [a]
Amorphous FeS	−2.93 [a]
αFeOOH goethite	14.97 [b]
FeCO$_3$ siderite	10.69 [c]
F1(OH)	4.33 [d]
F2(OH)	7.26 [d]
F1(Cl)	13.68 [d]
F2(Cl)	7.26 [d]
F1(SO$_4$)	6.82 [d]
F2(SO$_4$)	7.26 [d]

[a] Boulègue (1978).
[b] Detournay et al. (1975).
[c] Helgeson et al. (1969).
[d] Féder et al. (2005).

with temperature correction. The redox potential is calculated according to the rules explained in Bourrié et al. (1999). The activity of the electron is derived from the relation:

$$\log[e^-] = 2FE_{NHE}/(\ln RT)$$

where T is temperature (K), F, the Faraday constant ($F = 96,485$ C mol^{-1}) and R, the molar gas constant ($R = 8.31451$ J mol^{-1} K^{-1}).

After filtration at 0.2 μm, dissolved Fe (II) and total sulphurs were immediately analysed *in situ* by colorimetry with a portable spectrophotometer Hach DR/2010. Dissolved Fe(II) were analysed at 660 nm after di-2-pyridyl ketone benzoylhydrazone (DPKBH) complexation (Pehkonen et al., 1992 modified by Jaffrezic, 1997; Bourrié et al., 1999).

Sulphurous hydrogen and metallic sulphurs are soluble in acidic environments and react with *N,N*-dimethyl-*p*-phenylenediamine oxalate to form methylene blue. The measure is made at 665 nm.

Major and trace elements were analysed by ICP-AES and atomic absorption at the CEREGE in Aix-en-Provence (France) and anions by ionic chromatography (DIONEX) at the INRA unity of Aix-en-Provence (Géochimie des Sols et des Eaux). The relative precision is 2 to 5%.

2.3. Tests of mineral-solution balances

Thermodynamic calculations were made with species activities calculated by the Phreeqc model (Parkhurst and Appelo, 1999), based on the Debye–Hückel extended equation. It enables to calculate the distribution of solute chemical species at low temperature. pCO$_2$ and thermodynamic mineral-solution equilibria were calculated based on water analysis.

For iron oxides, Ionic Activity Products (IAP) are expressed as functions of the activity of the electron [e$^-$], the activity of Fe^{2+} and pH. The values of the solubility product in the standard conditions, K, are given in Table 1. The saturation state of the solution related to the mineral is interpreted according three different ways according to the Saturation Index (SI):

$$SI = \log IAP - \log K$$

The equilibrium is checked by plotting (SI):

- SI > 0: the solution is over-saturated relatively to the mineral;
- SI = 0: the solution is at equilibrium relatively to the mineral;
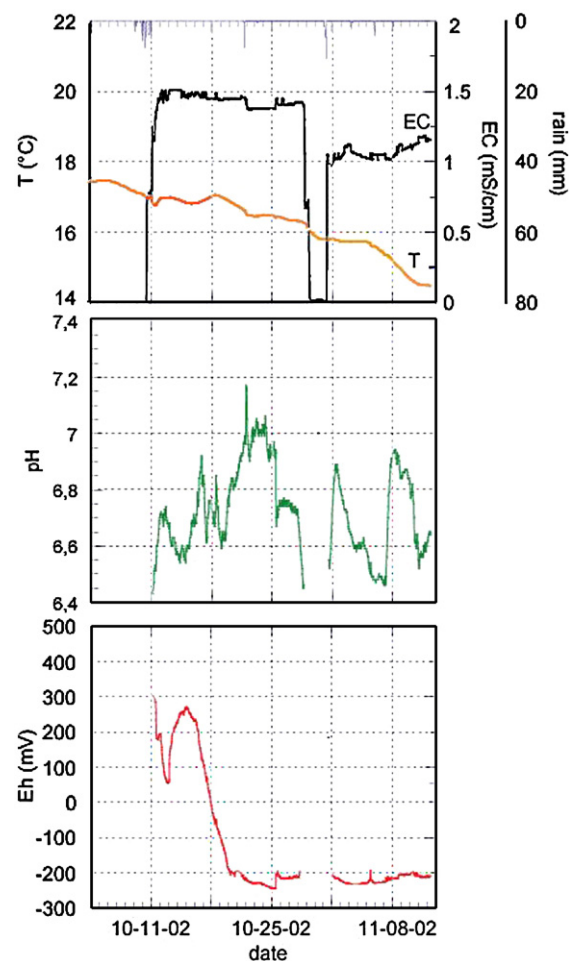- SI < 0: the solution is under-saturated relatively to the mineral;

Fig. 3. Physical and chemical parameters, *i.e.* T, EC, pH and Eh in the shallow groundwater at 1.1 m depth during a non-irrigated period in 2002.

Table 2
Concentrations of chemical elements in the paddy soil groundwater in mmol/L during the non-irrigated period in Autumn 2002 (dl: detection limit)

Date	Cl	Alk	Ca	NO$_3^-$	Fe(II)	Mn(II)	Al	Sulf tot	Sulphate	Mg	K	Na	Cu	Zn	Cr
10/03/02	5.87			0.069					5.8						
10/11/02	3.97	1.8	7.7	0.45	0.008	$2.5 \cdot 10^{-3}$	$5.2 \cdot 10^{-2}$	$1.6 \cdot 10^{-2}$	6.58	0.99	0.4	2.2	$2.6 \cdot 10^{-4}$	$1.7 \cdot 10^{-4}$	$1.9 \cdot 10^{-4}$
10/18/02	4.89			0.7	0.18				7.06						
10/25/02	6.05		6.5	<dl	0.23	$2.2 \cdot 10^{-3}$	$1.2 \cdot 10^{-2}$	$1.3 \cdot 10^{-3}$	6.47	1.52	0.62	2.29	$5.0 \cdot 10^{-5}$	$2.7 \cdot 10^{-4}$	$1.1 \cdot 10^{-4}$
11/05/02	3.26	2.5	5.05	0.051	0.041	$7.9 \cdot 10^{-3}$	$6.3 \cdot 10^{-2}$		4.84	1.4	0.63	1.93	$2.8 \cdot 10^{-5}$	$6.1 \cdot 10^{-4}$	
11/12/02	3.31	2.1	4.95	0.043	0.043	$5.4 \cdot 10^{-3}$	$3.1 \cdot 10^{-3}$	$4.1 \cdot 10^{-4}$	4.61	1.56	0.65	2.25		$3.4 \cdot 10^{-4}$	$1.3 \cdot 10^{-4}$
11/18/02	5.97		7.82	0.1	$9 \cdot 10^{-5}$	$5.6 \cdot 10^{-3}$	$8.1 \cdot 10^{-4}$	$3.2 \cdot 10^{-4}$	8.16	1.52	0.51	3.81	$8.2 \cdot 10^{-5}$	$7.3 \cdot 10^{-4}$	$1.3 \cdot 10^{-4}$
11/21/02	5.17			0.058	0.15				$6 \cdot 10^{-4}$	7.21					

2.4. X-Rays diffraction

X-Rays diffraction patterns were obtained with a Philips MPD 3710 at the CEREGE. The power of radiation is 40 kV, 40 mA and the source is a Co-Kα (1.79 Å). Rough soil samples are reduced in powder and directly analysed. In order to study clay minerals, the fraction inferior to 50 μm is submitted to 1% HCl and H_2O_2, in order to destroy respectively calcium carbonates and organic matter. To analyse iron oxides, micro-sampling was made.

2.5. DCB extractable Fe

Samples were extracted by Citrate–Bicarbonate (CB; Trolard, 1993; Trolard et al., 1995) and Dithionite Citrate Bicarbonate (DCB; Mehra and Jackson, 1960) to quantify iron oxides. DCB extracts all non-silicated Fe oxides, as it combines reduction by dithionite and complexation by citrate at pH buffered by bicarbonate. Structural iron in phyllosilicate minerals is not extractible by these reagents (Mitchell et al., 1971). Natural and synthetic green rusts are dissolved by CB within a few hours, while the other iron oxides are not dissolved (Trolard et al., 1996).

Samples were taken at 25, 50 and 80 cm at depth without any exposition to air and light. They were then introduced in a Jacomex/CEA glove box under nitrogen atmosphere to preserve the anoxic conditions of the samples, and to avoid any modification of clay behaviour by interaction with Fe(III) oxides. The reagents were prepared according to the procedure detailed in Féder
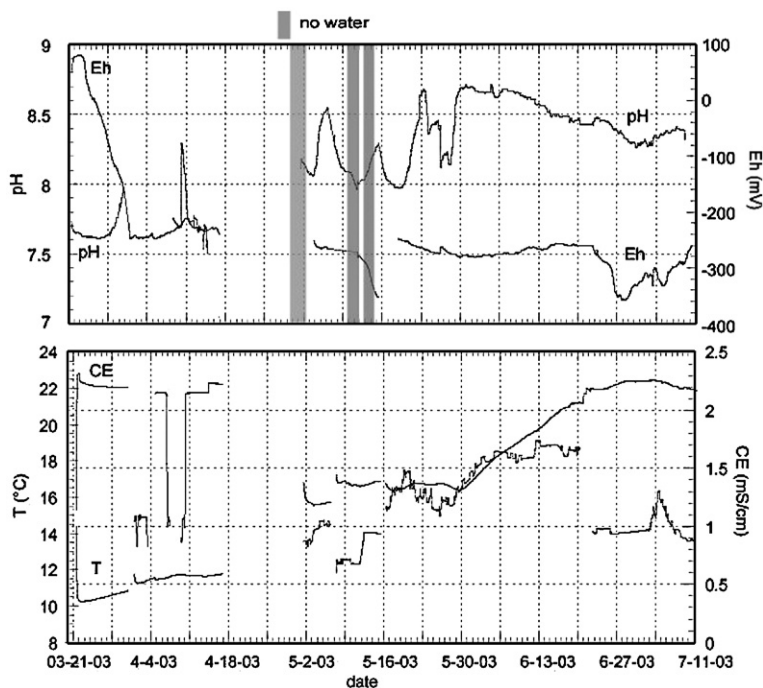

Fig. 4. Physical and chemical parameters, *i.e.* T, EC, pH, Eh in the shallow groundwater at 1.6 m depth during the irrigated period in 2003.

Table 3
Concentrations of chemical elements in the paddy soil groundwater in mmol/L during the irrigated period in Spring–Summer 2003

Date	Si	Cl	Alk	Ca	NO_3^-	NH_4^+	Fe(II)	Mn(II)	Sulf tot	Sulphate	Mg	K	Na	Cu	Zn
4/14/03	0.05	5.57			0.05	$1.3 \cdot 10^{-3}$		0.1		5.61	4.36	1.1	4.56	$1.6 \cdot 10^{-4}$	$6.1 \cdot 10^{-4}$
4/30/03		1.18		4.35	<dl	$1.1 \cdot 10^{-1}$		0.02	$4.1 \cdot 10^{-3}$	0.86	0.4	0.24	1.26	$1.6 \cdot 10^{-4}$	$1.1 \cdot 10^{-4}$
05/06/03	0.05	1.78		<dl		$1.9 \cdot 10^{-1}$				1.87					
05/15/03	0.02	2.66	3.6	3.87	0.06		0.25	0.03	$5.4 \cdot 10^{-3}$	2.58	0.96	0.67	2.95		<dl
06/04/03		3.31		6.5	0.16	$6.8 \cdot 10^{-3}$	0.09	0.02		4.38	2.12	0.56	2.92	$2.4 \cdot 10^{-5}$	$2.1 \cdot 10^{-4}$
06/12/03	0.02	2.97		65	0.07	$7.4 \cdot 10^{-3}$	0.05	0.02	$2.6 \cdot 10^{-4}$	4.01	1.18	0.83	2.83	$2.5 \cdot 10^{-4}$	$1 \cdot 10^{-4}$
06/20/03		1.95	6.9	3.75	0.01	$1.2 \cdot 10^{-1}$	0.06	0.03	$1.3 \cdot 10^{-3}$	2.04	0.96	0.41	4.75	<dl	$4.6 \cdot 10^{-4}$
06/27/03	0.05	1.76	6.76	3.95	<dl	$1.1 \cdot 10^{-1}$	0.06	0.01	$2.8 \cdot 10^{-2}$	1.56	0.84	0.35	1.6	$2.9 \cdot 10^{-4}$	$1.2 \cdot 10^{-4}$
07/03/03	0.19	2.31		3.91	<dl	$2.6 \cdot 10^{-3}$	0.02	0.02	$8.7 \cdot 10^{-2}$	1.47	0.85	0.88	1.8	$1.3 \cdot 10^{-4}$	$7.8 \cdot 10^{-4}$
07/09/03	0.14	1.71		3.5	0.03		0.04	0.01	$4.6 \cdot 10^{-2}$	1.08	0.80	0.37	1.67	$1.3 \cdot 10^{-4}$	$2.3 \cdot 10^{-4}$
07/22/03	0.11	1.04		<dl			0.01		$1.8 \cdot 10^{-4}$	0.37					
07/25/03		0.82			0.01					0.45					

et al. (2005). Analyses of Fe, Mg, Si, and Al were performed by ICP-AES.

3. Results

3.1. Groundwater analysis during a non-irrigated period

Fig. 3 and Table 3 present the evolution of the chemical and physical parameters of the groundwater. The piezometric level fluctuates between 60 and 160 cm depth. After equilibrium in fresh holes, the level rises 10–20 cm above the saturated zone. During some periods, the water table level was deeper than the measuring cell, and the conductivity is 0 mS/cm.

An important storm of 60 mm occurs on the 10th of October. Another less important rain event occurs on the 31st of October (Fig. 3). During the non-irrigated period in Autumn 2002, pH varies between 6.5 and 7.1 with large fluctuations.
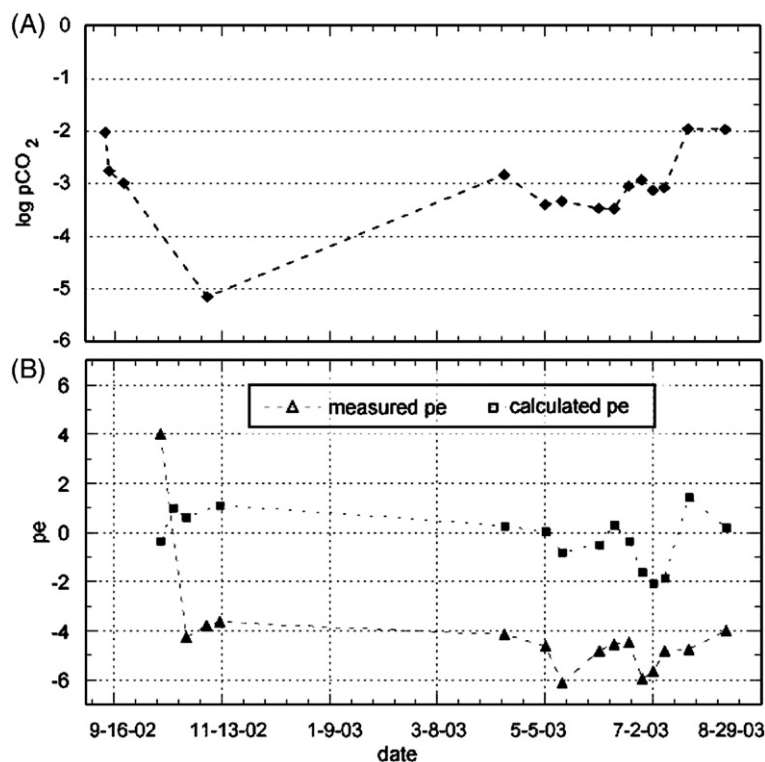

Fig. 5. (A): pCO$_2$ in function of time in the groundwater of the paddy soil and, (B): calculated or measured pe in the groundwater in 2002 and 2003.

The oxido-reductive potential is constant between −220 and −270 mV. The rainy event is followed by a high rise of Eh up to positive values (250 mV). During dry periods, dissolved Fe(II) concentrations are important (0.18 mmol/L on the 18th, 0.23 mmol/L on the 25th of October) (Table 2). One day after the storm, dissolved Al and trace metals have high concentrations but dissolved Fe and Mn concentrations reach the lowest values measured in 2002. Dissolved iron and manganese are correlated up to 97 %. During the non-irrigated period, the distribution of Cu, Zn and Cr is similar. The correlations between Fe and Cu and Zn are respectively 0.42 and 0.54. The system recovers its pre-storm physical and chemical values after 10 days.

3.2. Physical and chemical parameters during the irrigated period

During the irrigated period, the piezometric level is found constant at 40 cm depth whereas the saturated zone starts at 70 cm and the water level is at 80 cm depth. A non-saturated horizon is indeed sandwiched between two saturated zones, the water table and the irrigation-perched water table. It can be found either in Summer during irrigation or in winter.

Before the irrigated period in 2003, pH is rather constant at 7.6. After the inflow of irrigation water in the field, pH varies a lot, reaching 8.6 in June (Fig. 4). It decreases then slowly and constantly down to 8.2.
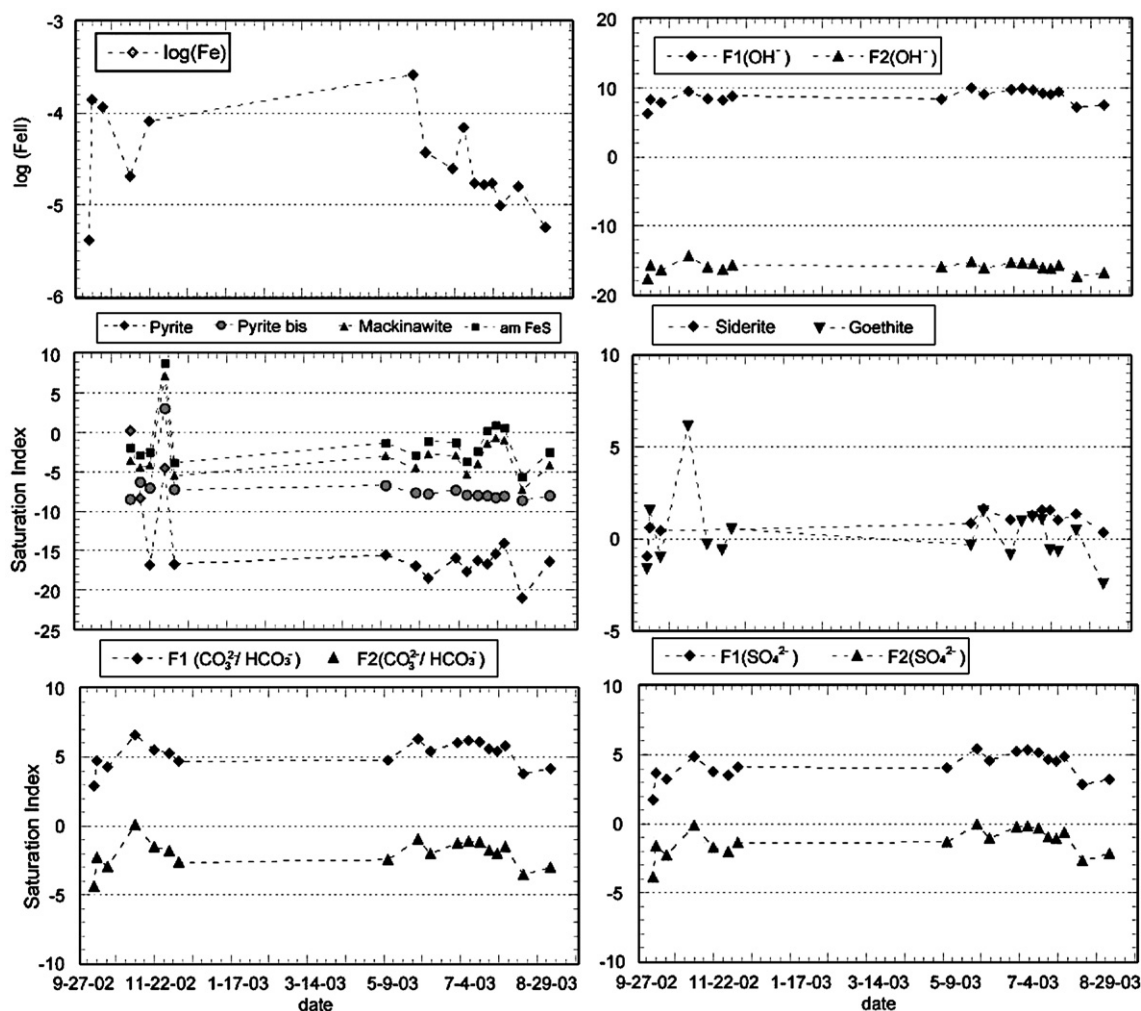

Fig. 6. Variations with time of the saturation index of groundwaters in the paddy soil relatively to iron oxides and fougerite with different anions (OH⁻, SO_4^{2-} or HCO_3^-/CO_3^{2-}) during irrigated and non-irrigated periods.
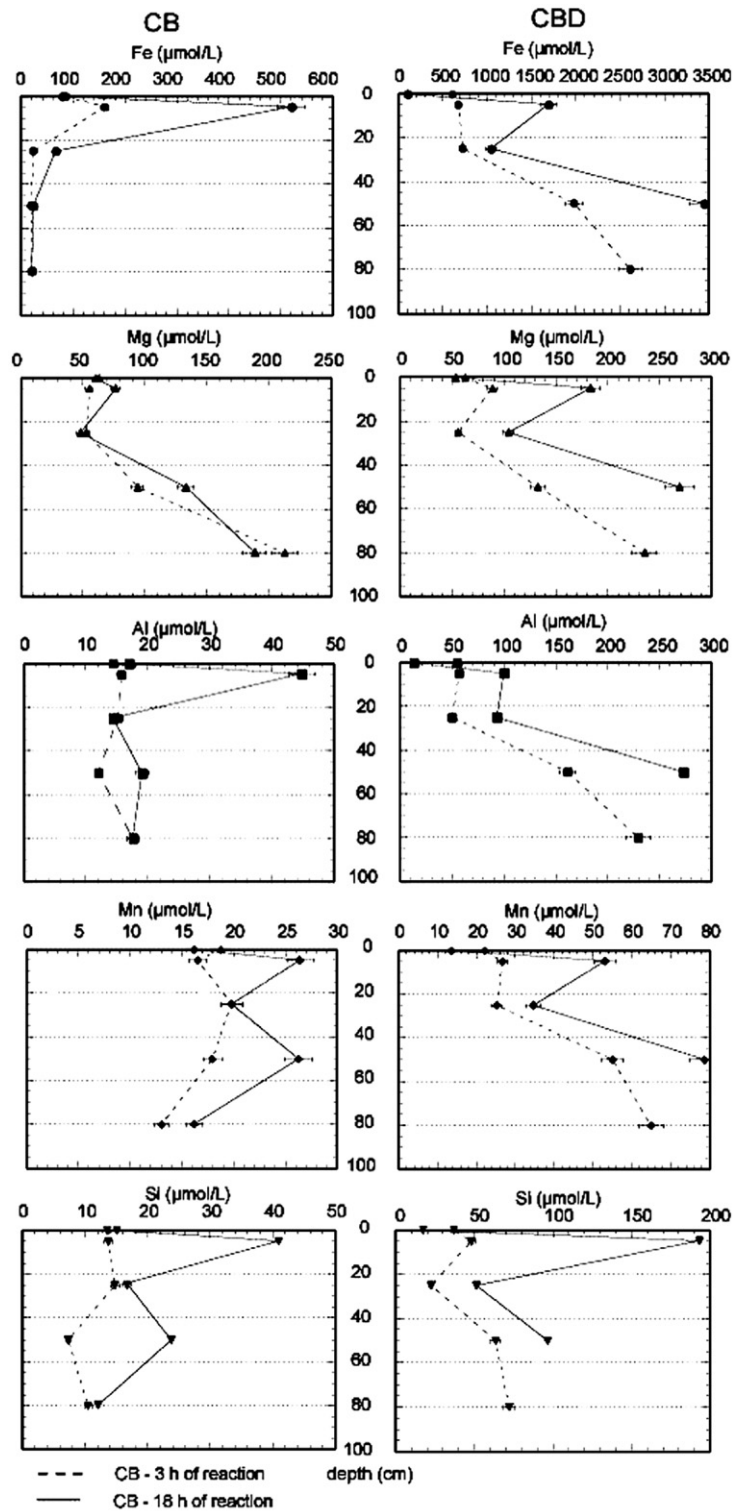
Fig. 7. Amounts of elements selectively extracted from iron oxides in the paddy soil in function of depth.

The oxido-reductive potential decreases regularly from −220 mV in April to −270 mV in June. Two important collapses down to −350 mV occur in May and June. In the beginning of July 2003, a high concentration of total dissolved sulphur (0.09 mmol/L) is measured (Table 3).

Between April and July, the concentrations of dissolved iron and manganese are respectively divided by 12 and 5. Iron is still well correlated to manganese (94 %). The concentrations of dissolved Zn and Cu are comparable to these in 2002 and are still very low.

pCO_2 and activities of siderite, goethite, fougerites, mackinawite and amorphous FeS are presented on Figs. 5 and 6. For pyrite and pyrite bis, two saturation indexes are given; the first one is calculated with pe measured on the field, and the second one according to the equation sulphate/sulphide:

$$1/8SO_4^{2-} + 9/8H^+ + e^- \Leftrightarrow 1/8HS^- + 1/2H_2O \\ \log K = 2.52 \tag{1}$$
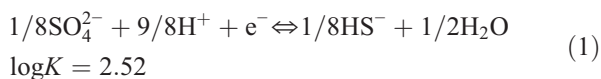
In fact, the potential of the electron, pe, calculated by Phreeqc is higher than the one measured on the field (Fig. 5). This is caused by the fact that the electrode is not sensible to the sulphate/sulphide couple and that the measured redox potential only depends on metallic couples as Fe^{2+}/Fe^{3+}, Fe^{2+}/iron oxides (s.l.), Fe^{2+}/sulphides… (Stumm and Morgan, 1970; Boulègue, 1978). Consequently, we suppose that only calculated pe are correct.

During the non-irrigated period, pCO_2 is close to $10^{-2.8}$ except for 1 day in November during which pCO_2 reaches 10^{-5}. During the irrigated period, pCO_2 firstly decreases down to $10^{-3.5}$ then increases up to 10^{-2}.

The variations of the saturation index in the groundwater are presented in Fig. 6. During both periods, the solution is balanced with goethite, and a little oversaturated regarding siderite. Soil solutions appear either oversaturated or undersaturated with respect to OH-fougerite and carbonate-fougerite. It is close to saturation with F2-sulphate although it is oversaturated with F1-sulphate. The solution is largely undersaturated with Cl-fougerite (result not showed). At the beginning of July 2003, the solution appears punctually at equilibrium with amorphous sulphurs.

3.3. Iron oxides kinetic dissolution

Fig. 7 presents the amount of elements selectively extracted from iron oxides in function of depth. The CBD pool always has more important amounts of extracted elements than the CB pool. The most CB-extracted and CBD-extracted element are respectively Mg and Fe. The difference between CBD and CB gives evidence of the presence of crystallized iron oxides as goethite and of a Fe–Mn–Al–Mg–Si phase more crystallized than over the plough sole.

4. Discussion

4.1. Factors leading to Eh variations and metal mobility

4.1.1. Oxide dissolution during short time event

Sharp and fast Eh fluctuations are observed after storms at quasi-constant pH. The system modification never last more than 2 weeks. These redox fluctuations can be explained by oxygen input by rainwater rich in atmospheric O_2. In these conditions, goethite is stable and its presence has been assessed by X-Rays diffraction (Cary, 2005). Although lepidocrocite should be also stable in these conditions, it is not taken into account because the presence of carbonate is not in favour of its precipitation (Schwertann and Fechter, 1994). The concentrations of dissolved trace elements are high when the concentration of dissolved Fe(II) and Mn(II) are low. This result is different from the one obtained by Trolard et al. (2002) who showed that the dynamics of Cu and Zn are closely linked to the Fe one. We suppose then that iron and manganese oxides submitted to dissolution do not contain sufficient amounts of trace metal to affect the solution.

4.1.2. Impact of sulphate/sulphur presence during the irrigation period

Two periods of sharp decrease of Eh linked to pH decrease happen, the second one being linked with sulphur production and sulphate decrease. When Eh is inferior to −120 mV, all sulphates should be reduced in sulphurs according to the equation:

$$1/8SO_4^{2-} + 9/8H^+ + e^- \Leftrightarrow 1/8HS^- + 1/2H_2O \tag{2}$$
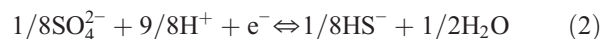
The presence of sulphates during all periods can be explained by the vicinity of the sea but can also indicate a system which has not reached its equilibrium. Moreover, to such Eh in absence of oxygen, Fe^{2+} predominates. Consequently, Fe^{2+} and HS^- can be both simultaneously dissolved. The precipitation of amorphous iron sulphurs and the production of protons is then possible according to the equation:

$$Fe^{2+} + HS^- \Leftrightarrow FeS + H^+, \log K = 2.93 \tag{3}$$
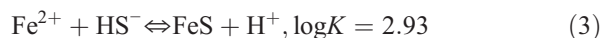
(Boulègue, 1978) This phenomenon is well foreseen by thermodynamic calculations (Fig. 6). The system recovers quickly its usual Eh values.

4.2. Factors leading to pH variations and metal mobility

4.2.1. Soil acidification during a short time event

Fast geochemical phenomena can happen in groundwaters at 1.1 m depth under a plough sole. The amplitude of pH oscillations after the October storm (0.2 to 0.4 pH unity) implies that the carbonated system is not enough buffered to keep a stable pH. A previous work (Cary and Trolard, 2006) has showed that in the carbonated system, the soil solution appears undersaturated with respect to calcite, dolomite and magnesite during a non-irrigated period.

Soil acidification induces oxide and oxi-hydroxide dissolutions that can buffer a pH decrease. For example, goethite dissolution liberates hydroxide ions:

$$FeOOH + H_2O \Leftrightarrow Fe^{3+} + 3OH^- \qquad (4)$$

Just after the storm, a peak of nitrates occurs with a pH close to 6.6. This may be due (i) by nitrate entry with rain water and (ii) by the oxidation of NH_4^+ by the oxygen in the rain water according to the two half equations:

$$O_{2g} + 4H^+ + 4e^- \rightarrow 2H_2O \qquad (5)$$

$$NH_4^+ + 3H_2O \rightarrow NO_3^- + 10H^+ + 8e^- \qquad (6)$$

resulting in the oxido-reduction equation:

$$NH_4^+ + 2O_{2g} \Leftrightarrow NO_3^- + 2H^+ + H_2O \qquad (7)$$

Féder et al. (2005) recorded sharp pH variations close to one pH unity in Fougères. This difference can be mainly explained by the different inner conditions of the system: in Fougères, the probe was put at 70 cm depth in a non-carbonated soil catena of cambisols and gleysols.

4.2.2. Mineral precipitation during long time event

During long periods where reduced conditions prevail, the amount of CO_2 in solution controls sharp pH variations which control oxido-reductive processes. The frequency of redox shifts then influences soil mineral transformation, by allowing the co-precipitation of mineral phases constituted by Fe, Mn, Al, Mg and Si.

Sharp pH increases are observed during irrigation at quasi-constant Eh. In May, the first increase of pH from 8 to 8.5 at constant Eh (-270 mV) can be due to the sum of two phenomena: (i) the pH of the irrigation water is close to 8.5 until the end of May (Cary, 2005) and (ii) as iron oxides are able to precipitate, Fe^{2+}, and to some extent Mn^{2+}, do not contribute anymore to the solution alkalinity.

Started in May, the slow decrease of pH can be explained by the formation of iron oxides. Thermodynamics calculations indicate that the solution is close to saturation with goethite and F2-sulphate during a period in May and June 2003. The formation of the mineral produces H^+ according to the equation (Féder et al., 2005):

$$5/9Fe^{2+} + 4/9Mg^{2+} + 1/6SO_4^{2-} + 2H_2O \Leftrightarrow F2 \\ + 1/3e^- + 2H^+ \qquad (8)$$
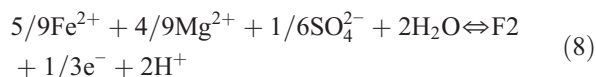
In the same way, the precipitation of goethite and Mn oxide produces protons according to the following equations:

$$Fe^{2+} + 2H_2O \Leftrightarrow \alpha FeOOH + 3H^+ + e^- \qquad (9)$$

$$Mn^{2+} + 2H_2O \Leftrightarrow MnOOH + 3H^+ + e^- \qquad (10)$$
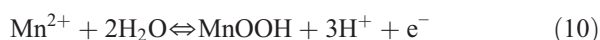
This driving of oxido-reduction processes by pH has already been observed by Féder et al. (2005) in a system where pH oscillations may be superior to 1 unity pH.

As the saturation index of goethite varies according to the concentration of Fe^{2+} (Fig. 6), goethite, which exists in the soil, may be able to control dissolved Fe(II) concentrations.

The precipitation of iron and manganese oxides may not make pH decrease under 8. But the system being carbonated, iron and manganese carbonates and thus pCO_2 must be considered. Indeed, thermodynamic calculations show that siderite could precipitate in the groundwater. According to Kirk (2004) and Deer et al. (1992), it is probable that amorphous Fe–Mn carbonates incorporating Mg^{2+} shall be found in the soil because siderite and rhodocrosite are the end-members of continuous series of solid-solutions of Fe(II)–Mn(II) carbonates.

Moreover, selective dissolutions of iron oxides give evidence of the presence of crystallized iron oxide as goethite and of an undetermined crystallized Fe–Mg–Mn–Al–Si phase. This result is reinforced by the recent work of Thompson et al. (2006) who showed that several consecutive redox cycles make the crystalline character of Fe-minerals increase from nano- to micro-Fe oxides which can be submitted to metal substitution. We can suggest that the crystalline character, the size and the quantity of Fe-minerals at the vicinity of the water-table level may have increase during these last 30 years in the paddy soil redox-dynamic environment.

5. Conclusion

In the groundwater of a paddy soil in Camargue, different events as a storm or irrigation induce very sharp physical and chemical variations by modifying the

aeration and the aerobic and anaerobic conditions. These modifications can be very fast and are thus only perceptible with accurate tools on the field, *i.e.* continuous and *in situ* analyses. They prove how reactive a redox-dynamic environment can be. It can be enhanced that (i) Eh variations happens at quasi-constant pH during Mediterranean storms in non-irrigated Summer and Autumn, and (ii) there exist long periods where the soil is saturated with water in reducing conditions, and where sharp pH variations control oxido-reduction processes but are controlled by the amount of CO_2 in solution. During the irrigated period, it seems likely that neoformed Fe and Mn oxides will precipitate thanks to pH control. During the non-irrigated period, the dissolution of Fe and Mn oxides does not affect the concentrations of trace metals. An oxido-reductive zone develops in the vicinity of the water table level.

In case of a complete change of agricultural practices, as for example the end of irrigation, these oxides may be submitted to complete dissolution in a short period of time. Even if there seems to be no threat of metal pollution in actual conditions, the understanding of the fast reactivity of a system helps to better assess the environment durability.

Acknowledgments

References

Astier, 1970. Collectif Camargue. Etude hydrogéologique, pédologique et de salinité. DDA et CNA du Bas-Rhône et du Languedoc-Arles.

Boivin, P., Favre, F., Hammecker, C., Maeght, J.L., Delariviere, J., Poussin, J.C., Wopereis, M.C.S., 2002. Processes driving soil solution chemistry in a flooded rice-cropped vertisol: analysis of long time monitoring data. Geoderma 110, 87–107.

Boulègue, J., 1978. Géochimie du soufre dans les milieux réducteurs. Paris. 272 pp.

Bourrié, G., Trolard, F., Genin, J.-M.R., Jaffrezic, A., Maître, V., Abdelmoula, M., 1999. Iron control by equilibria between hydroxy-Green Rusts and solutions in hydromorphic soils. Geochimica et Cosmochimica Acta 63 (19/20), 3417–3427.

Cary, L., 2005. Mobilité des éléments selon les alternances aérobie–anaérobie dans un écosystème rizicole en Camargue, Thèse de l'Université Paul Cézanne, Aix-Marseille III, 275 pp.

Cary, L., Trolard, F., 2006. Effects of irrigation on geochemical processes in a paddy soil and in groundwaters in Camargue (France). Journal of Geochemical Exploration 88, 177–180.

Chauvelon, P., 1996. Hydrologie quantitative d'une zone humide méditerranéenne aménagée: le bassin de Fumemorte en Grande Camargue, delta du Rhône. 267 pp.

Deer, W.A., Howie, R.A., Zussman, J., 1992. An Introduction to the Rock-Forming Minerals. Longman Scientific and Technical, Harlow.

Detournay, J., De Miranda, L., Derie, R., Ghodsi, M., 1975. The region of stability of green rust II in the electrochemical E-pH equilibrium diagram of iron in sulphate medium. Corrosion Science 15, 295–306.

F.A.O., 1999. World Reference Base. Note 84. ISSN 1014-8531.

Féder, F., Trolard, F., Klingelhofer, G., Bourrié, G., 2005. In situ Mössbauer spectroscopy — evidence for green rust (Fougérite) in a gleysol and its mineralogical transformations with time and depth. Geochimica et Cosmochimica Acta 68 (18), 4463–4483.

Helgeson, H.C., Garrels, R.M., Mackenzie, F.T., 1969. Evaluation of irreversible reactions in geochemical processes involving aqueous solutions. Geochimica et Cosmochimica Acta 33, 569–592.

Heurteaux, P., 1990. Les phénomènes hydrauliques souterrains induits par la riziculture en Camargue: conséquences écologiques et agronomiques, Centre Français du Riz.

Hossain, M.F., 2006. Arsenic contamination in Bangladesh — an overview. Agriculture, Ecosystems and Environments 113, 1–16.

Jaffrezic, A., 1997. Géochimie des éléments métalliques, des nitrates et du carbone organique dissous dans les eaux et les sols hydromorphes. Agriculture intensive et qualité des eaux dans les zones humides en Bretagne. Mémoire, vol. 79. Géosciences Rennes, Rennes.

Kirk, G., 2004. The Biogeochemistry of Submerged Soils, vol. 1. John Wiley.

L'homer, A., Bazile, A., Thommeret, J., 1981. Principales étapes de l'édification du delta du Rhône de 7000 BP à nos jours; variations du niveau marin. Oceanis 7 (4), 389–408.

Meharg, A.A., 2004. Arsenic in rice — understanding a new disaster for South-East Asia. Trends in Plant Science 9 (9), 415–417.

Mehra, O., Jackson, M., 1960. Iron oxides removal from soils and clays by a dithionite–citrate system buffered with sodium bicarbonate. Clays and Clay Minerals 7, 317–327.

Mitchell, B.D., Smith, B.F.L., Endredy, A.S., 1971. The effect of buffered sodium dithionite solution and ultrasonic agitation on soil clays. Israelian Journal of Chemistry 9, 45–52.

Parkhurst, D.L., Appelo, C.A.J., 1999. User's guide to PHREEQC (version 2) — a computer program for speciation, batch-reaction, one-dimensional transport and inverse geochemical calculations. Water-Resources Investigations, Denver, Colorado.

Pehkonen, S., Eyrel, Y., Hoffman, M., 1992. Simultaneous spectrophotometric measurement of Fe(II) and Fe(III) in atmospheric water. Environmental Science and Technology 26 (9).

Polizzotto, M.L., Harvey, C.F., Li, G., Badruzzman, B., Ali, A., Newville, M., Sutton, S., Fendorf, S., 2006. Solid-phases and desorption processes of arsenic within Bangladesh sediments. Chemical Geology 228 (1-3), 97–111.

Ponnamperuma, F.N., 1972. The chemistry of submerged soils. Advances in Agronomy 29–96.

Ponnamperuma, F.N., Tianco, E.M., Loy, T., 1967. Redox equilibria in flooded soils: I. The iron hydroxide system. Soil Science 103, 374–381.

Revil, A., Cary, L., Fan, Q., Fininzola, A., Trolard, F., 2005. Self-potential signals associated with preferential groundwater flow pathways in a buried paleo-channel. Geophysical Research Letters 32 (7).

Rossiaud, J., 1994. Réalités et imaginaires d'un fleuve, Université de Paris 1, Panthéon Sorbonne.

Schwertann, U., 1988. Occurrence and formation of iron oxides in various pedoenvironments. In: Stucki, J.W., et al. (Ed.), Iron in Soil

and Clay Minerals, NATO Series. Dordrecht Reidel Publishing Company, pp. 715–748.

Schwertann, U., Fechter, H., 1994. The formation of green rust and its transformation to lepidocrocite. Clays Minerals 29, 87–92.

Stucki, J.W., 1988. Structural iron in smectites. In: Stucki, J.W., et al. (Ed.), Iron in Soil and Clay Minerals, NATO Series. Dordrecht Reidel Publishing Company, pp. 625–675.

Stumm, W., Morgan, J., 1970. Aquatic Chemistry. Wiley — Interscience.

Sposito, G., 1981. The Thermodynamics of Soil Solutions. Oxford University Press, Oxford, UK.

Thompson, A., A., C.O., Rancourt, D., Chorover, J., 2006. Iron-oxide crystallinity increases during soil redox oscillations. Geochimica et Cosmochimica Acta 70 (7), 1710–1727.

Trolard, F., 1993. Les formes solides du fer en milieu hydromorphe acide : une approche compartimentale par dissolution sélective. Comptes Rendus de l'Academie des Sciences 316 (II), 1463–1468.

Trolard, F., Bourrié, G., Jeanroy, E., Herbillon, A.J., Martin, H., 1995. Trace metal in natural iron oxides from laterites: a study using selective kinetic extraction. Geochimica et Cosmologica Acta 59 (7), 1285–1297.

Trolard, F., Abdelmoula, M., Bourrié, G., Humbert, B., Genin, J.-M.R., 1996. Mise en évidence d'un constituant de type "rouilles vertes" dans les sols hydromorphes. Proposition de l'existence d'un nouveau minéral: la "fougérite". Comptes Rendus de l'Academie des Sciences Paris 323 (série II a), 1015–1022.

Trolard, F., Bourrié, G., Soulier, A., Maître, V., Genin, J.-M.R., Abdelmoula, M., 1998. Dynamique de l'oxydo-réduction dans les zones humides. In: Cheverry, C. (Ed.), Agriculture intensive et qualité des eaux. INRA Editions, Paris, pp. 185–199.

Trolard, F., Bourrié, G., Jaffrezic, A., 2002. Distribution spatiale et mobilité des ETM en région d'élevage intensif. In: Baize, D., Tercé, M. (Eds.), Les éléments traces métalliques dans les sols. INRA, Paris.

Turner, F.T., Patrick, W.H.J., 1968. Chemical changes in waterlogged soils as a result of oxygen depletion. In: Holmes, J.W. (Ed.), IXth International Congress of ISSS. Transactions, IV ISSS and Angus and Roberston ltd, Sydney, Adelaide, pp. 53–65.

Van Cappellen, P., Viollier, E., Roychoudhury, A., Clark, L., Ingall, E., Lowe, K., Dichristina, T., 1998. Biogeochemical cycles of manganese and iron at the oxic-anoxic transition of a stratified marine basin (Orca Basin, Gulf of Mexico). Environmental Science & Technology 32, 2931–2939.

Van Geen, A., Zheng, Y., Cheng, Z., He, Y., Dhar, R.K., Garnier, J.M., Rose, J., Seddique, A., Hoque, M.A., Ahmed, K.M., 2006. Impact of irrigating rice paddies with groundwater containing arsenic in Bangladesh. Science of the Total Environment 367 (2–3), 769–777.